



Published in final edited form as:

*Curr Res Biotechnol.* 2021 ; 3: 288–299. doi:10.1016/j.crbiot.2021.11.003.

## Highly portable quantitative screening test for prostate-specific antigen at point of care

Balaji Srinivasan<sup>a,b</sup>, David M. Nanus<sup>d</sup>, David Erickson<sup>a,b,c</sup>, Saurabh Mehta<sup>a,b,\*</sup>

<sup>a</sup>Division of Nutritional Sciences, Cornell University, Ithaca, NY 14853, USA

<sup>b</sup>Institute for Nutritional Sciences, Global Health, and Technology (INSiGHT), Ithaca, NY, USA

<sup>c</sup>Sibley School of Mechanical and Aerospace Engineering, Cornell University, Ithaca, NY, USA

<sup>d</sup>Division of Hematology and Medical Oncology, Department of Medicine, Weill Cornell Medicine, New York, NY, USA

### Abstract

Prostate cancer (PCa) is the second most diagnosed cancer among men. Targeted PCa screening may decrease PCa-specific mortality. Prostate-specific antigen (PSA) is the most reliable and widely accepted tumor biomarker for screening and monitoring PCa status. However, in many settings, quantification of serum PSA requires access to centralized laboratories. In this study, we describe a proof-of-concept rapid test combined with a highly portable Cube™ reader for quantification of total PSA from a drop of serum within 20 min. We demonstrated the application of gold nanoshells as a label for lateral flow assay with significant increase in the measured colorimetric signal intensity to achieve five times lower detection limit when compared to the traditionally used 40 nm gold nanosphere labels, without a need for any additional signal amplification steps. We first optimized and evaluated the performance of the assay with commercially available total PSA calibrators. For initial validation with commercially available ACCESS Hybritech PSA calibrator, a detection range of 0.5–150 ng/mL was achieved. We compared the performance of our total PSA test with IMMULITE analyzer for quantification of total PSA in archived human serum samples. On preliminary testing with archived serums samples and comparison with IMMULITE total PSA assay, a correlation of 0.95 ( $p < .0001$ ) was observed. The highly portable quantitative screening test for PSA described in this study has the potential to make PCa screening more accessible where diagnostic labs and automated immunoassay systems are not available, to reduce therapeutic turnaround time, to streamline clinical care, and to direct patient care for both initial screening and for post-treatment monitoring of patients.

This is an open access article under the CC BY-NC-ND license (<http://creativecommons.org/licenses/by-nc-nd/4.0/>).

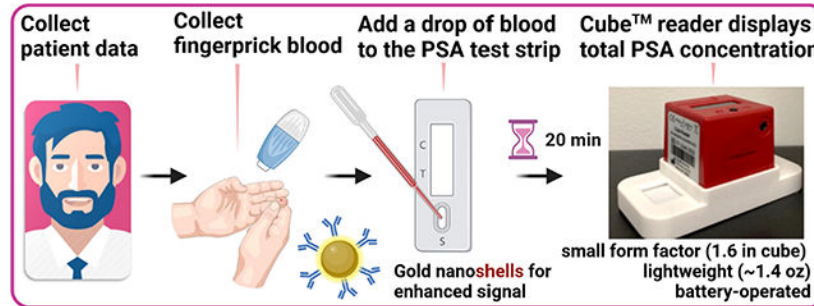
\*Corresponding author at: Division of Nutritional Sciences, Cornell University, Ithaca, NY, USA. [smehta@cornell.edu](mailto:smehta@cornell.edu) (S. Mehta). Author contributions

BS and SM conceptualized and designed the study. BS performed assay development, experimental work, data analysis, and drafted the initial manuscript. DMN, DE, and SM supervised the overall study. All authors reviewed, revised, and approved the final version of the manuscript.

#### Declaration of Competing Interest

The authors declare the following financial interests/personal relationships which may be considered as potential competing interests: DE and SM have an equity interest in VitaScan Technologies, Inc., that aims to commercialize point-of-care assays for nutritional status developed in their research laboratories. The remaining authors have no financial relationships relevant to this article to disclose.

## Graphical Abstract



## Keywords

Prostate cancer; Screening; Point of care; POCT; Prostate-specific antigen; Cancer

## 1. Introduction

Prostate cancer (PCa) is the second most diagnosed cancer among men with annually estimated 1,400,000 new cases worldwide (Sung et al., 2021). In the United States, PCa accounts for 26 percent of cancer diagnoses (Siegel et al., 2021) and is the leading cause of cancer in men. PCa mortality rates have declined in the United States, decreasing from 39 to 19 per 100,000 persons during 1992–2017 (Noone et al., 2017). Mathematical models indicate that screening accounts for 45–70 percent of the decline in PCa, and mainly by decreasing the incidence of men diagnosed with advanced stage disease (Etzioni et al., 2008). Prostate-specific antigen (PSA) is the most reliable and widely accepted tumor biomarker for screening and monitoring prostate cancer status (So et al., 2003). In the U.S., the PCa mortality rate declined by 39% from 1991 to 2008, with the decrease attributed in part to early detection by screening based on the PSA test (Brawley, 2012). However, PSA testing frequency has declined across all racial/ethnic groups in the US over the past decade with the rate of decline modestly steeper among African American (AA) men, and particularly AA men aged 40–54 (Kensler et al., 2021). Studies suggest that there are racial differences in beliefs and attitudes around PCa screening. More effective communication between physicians and AA men regarding PSA screening may increase the number of patients who undergo screening (Miller et al., 2021; Woods-Burnham et al., 2018). Another impediment may be that AA men are less likely to have accessible health care and may not go for routine medical care (Nelson et al., 2021). In one study, 42.9% of AA men aged 41 or older had never had a PSA test, and most of them chose to have a PSA test at a health fair (Hewitt et al., 2018). It is, therefore, imperative to reach this group outside of the health care system.

The Food and Drug Administration (FDA) approved the determination of PSA serum levels to test asymptomatic men for prostate cancer, in conjunction with digital rectal exam (DRE), in men aged 50 years old or older with a serum PSA cut-off value of 4 ng/ml. The US Preventive Services Task Force (USPSTF) recommends that men aged 55 to 69 years should consider undergoing periodic PSA-based screening for PCa including a discussion

of the potential benefits and harms of screening with their physician (USPSTF, 2018). Even though the best cutoff to predict PCa based on serum PSA concentrations has been debated, historically a concentration below 4 ng/mL is usually considered healthy in most cases. Age-specific (Partin et al., 1996) and race-specific (Morgan et al., 1996) reference values for PSA have been proposed but are rarely followed in clinical practice. Besides initial screening for PCa, periodic PSA tests are also routinely used to monitor disease progression and inform clinical decision making after diagnosis and treatment of PCa.

At present, most PSA tests are performed at dedicated centralized laboratories on large automated high throughput immunoanalyzers. Some of these commercial immunoanalyzers available for quantification of PSA include - Roche Cobas® Core PSA Total enzyme immunoassay (EIA), Elecsys® total PSA, Simoa™ Total PSA (Quanterix™), Immulite 2000 XPI (Siemens Healthcare Diagnostics Inc., Tarrytown, NY, USA), UniCel DxI 800 (Beckman Coulter, Brea, CA, USA), ADVIA Centaur XPT (Siemens Healthcare Diagnostics Inc.), and ARCHITECT i2000SR (Abbott Diagnostics, Abbott Park, IL, USA). There are numerous advantages to these fully automated analyzers, including lower detection limits (0.05–0.005 ng/ml range), reliability and high-throughput of samples. However, an important limitation is that these analyzers are suitable for dedicated laboratories and not readily available in the community.. Also, sample transportation requirement causes delays, and the therapeutic turnaround time (Kost, 1995), which is the time between the decision to test and the therapeutic action taken on the test result, is typically of the order of a few days. These limitations also prevent tPSA screening in resource-limited settings that lack access to centralized laboratories with fully automated analyzers. At present there are no Food and Drug Administration (FDA) -approved lateral flow test strips available in the US market for PCa screening based on serum total PSA (tPSA) quantification. At-home PSA tests such as ‘PSA micro™’ from Pinnacle BioLabs (Nashville, TN) are available, but require collection of 3–4 drop of blood to be sent to the lab for processing. Recently, the FDA approved the Sangia Total PSA Test (OPKO Diagnostics), which includes a microfluidic cassette with Claros® 1 bench-top analyzer diagnostic instrument system to quantify tPSA from a drop of blood. However, currently there is no information on OPKO’s website as to if and when this will be commercially available in the US.

In recent years, the development of biosensors that have the potential for use in point-of-care testing (POCT) devices are revolutionizing medical diagnostics. These POCT biosensors are designed to provide rapid and reliable quantitative results ‘anytime, anywhere’ the patient is. For POCT to be more widely used, there is interest in reducing the current assay formats to the size of portable, handheld devices requiring small sample volumes and reagents consumed, while providing a specific and sensitive assay comparable to laboratory standard analyzers. Recent advances in using nanoparticles and nanostructures as integral components, have enabled the development of highly miniaturized microfluidic techniques for analyte detection. The most common microfluidic techniques previously reported to quantify serum tPSA at the point-of-care include Surface Plasmon Resonance (SPR) (Ertürk et al., 2016; Uludag and Tothill, 2012), Surface Enhanced Raman Scattering (SERS) (Chang et al., 2016), fluorescence assay (Barbosa et al., 2014; Kong et al., 2015; Pei et al., 2015), electrochemical impedance spectroscopy (EIS) (Chornokur et al., 2011; Gutiérrez-Zúñiga and Hernández-López, 2014; Yan et al., 2012), cyclic voltammetry (CV)

(Dong et al., 2017; Kavosi et al., 2014; Rafique et al., 2015), electrochemiluminescence (ECL) (Wu et al., 2016), amperometric (Wu et al., 2016), capacitance (Ertürk et al., 2015) and photo-electrochemical (PEC) (Wang et al., 2017; Zhang et al., 2017). These microfluidic techniques provide the required detection ranges, limit of detection, and time-to-result. However, most of these devices require complex and expensive microfabrication methods that limit rapid product development from laboratory prototypes. Other drawbacks are the requirement of additional equipment to power the device and measure the output signal, and active control of the fluid flow within the device. In recent years, to rapidly identify biologically active compounds, immunochromatographic assay techniques are widely used to overcome the limitations of other microfluidic devices. Immunochromatographic assays are now gaining wider use as a quantitative method over their mostly qualitative testing approach during the early years of development. Immunochromatographic methods are characterized by small sample volume (~20 µL), shorter time-to-result (10–20 min), and analysis that does not require expensive equipment or highly trained personnel. Immunochromatographic method enables screening at the point-of-care with high sensitivity, visual and quantitative interpretation of the results, and low cost. The most common immunochromatographic configuration is the lateral flow immunoassay (LFIA) (Posthuma-Trumpie et al., 2009), more commonly referred to as a test strip, in which gold nanoparticle labels are often applied to provide colorimetric signal quantification of results. Gold nanoparticle of various shape and volume including nanospheres, nanorods, nanowires, and nanocubes are commercially available and have been reported in numerous lateral flow assays. Selection of the label is critical for the performance of any lateral flow assay. The most common nanoparticle used in commercial lateral flow assay is 40 nm gold nanosphere due to its optimal combination of high contrast color (absorption ~ 523 nm) with distinct cherry red color for visual readouts and surface area suitable for targeting analytes of wide size ranges. In this study, we compared the performance of gold nanoshells with the widely used, industry standard 40 nm gold nanospheres. The structure of gold nanoshells consist of a 110 nm core silica sphere with thin (12–18 nm) gold shell deposited over it. The silica core reduces the overall particle density relative to a solid gold nanosphere of same size, allowing for improved flow rates through a lateral flow membrane compared to a 150 nm solid gold sphere (Nanocomposix, 2021). Gold nanoshells produces a high contrast blue-grey line that is clearly visible.

In recent years, lateral flow immunoassays have been coupled with smartphones (Foyosal et al., 2019; Lee et al., 2016) and battery powered portable readers (Srinivasan et al., 2018) for imaging the test strips at the point of care. Lateral flow test strips rely on capillary flow within nitrocellulose membrane without any need for external pump or moving components to control the flow. LFIA for PSA based on gold nanoparticle (Andreeva et al., 2016), quantum dot nanobeads (Li et al., 2014), and fluorescent Europium labels (Juntunen et al., 2012) have been reported. However, at present, FDA approved LFIA for PSA is not commercially available. We hypothesized that providing PCa screening using a near-patient tPSA test performed by a fingerstick blood draw in combination with a portable handheld reader, will be cost-effective (< \$1 per test), provide results within 20 min, and increase screening rates within community settings. There is an urgent need for a near-patient or POCT to reduce the frequency of clinical visits by the patients, cost-effectiveness, streamline

clinical care for the urologist and patient, improve patient satisfaction and clinical outcome by enabling rapid decision making.

## 2. Materials and methods

### 2.1. Reagents and materials

Gold nanoshells (Bioready 150 nm Carboxyl Gold nanoshell) was purchased from nanoComposix (San Diego, CA). Gold nanoparticle conjugation kit (Gold Conjugation Kit 40 nm, 20 OD cat# ab154873) was purchased from Abcam (Waltham, MA). Monoclonal antibodies mouse anti-human-PSA (cat# MP077, clone BP005S for capture and clone AP002S for detection) and colloidal gold conjugate stabilizer (cat# 90092-0100) were purchased from Scripps Laboratories (San Diego, CA). Secondary antibody (AffiniPure Goat Anti-Mouse IgG, cat# 115-005-146) was purchased from Jackson ImmunoResearch Laboratories Inc. (West Grove, PA). ACCESS Hybritech tPSA calibration kit (cat# 37205) was purchased from Beckman Coulter (Brea, CA). Amine free phosphate buffer saline (PBS) buffer pH 7.4, 50% (w/v) hydroxylamine, sulfo-N-hydroxysuccinimide (sulfo-NHS), 1-Ethyl-3-(3-dimethylaminopropyl) carbodiimide hydrochloride (EDC), 2-(N-morpholino) ethanesulfonic acid (MES) buffer, Polyethylene glycol-20 k (PEG 20 k), sodium azide, casein solution, potassium phosphate buffer, Tween-20, and bovine serum albumin (BSA) were acquired from Sigma-Aldrich (St. Louis, MO, USA). Samples of membrane sheets - conjugate pad (cat# 8980), sample pad (cat# 8981), absorption pad (cat# 440) were provided by Ahlstrom-Munksjö (Mt. Holly Springs, PA). Nitrocellulose membrane (Unisart® CN 140, 30 mm wide) was purchased from Sartorius Stedim Biotech GmbH (Göttingen, Germany). Masking tape (cat# MT2) and blood separation membrane (cat# FR1(0.6)) were purchased from Advanced Microdevices Pvt. Ltd. (MDI) (Camp Hill, PA). Backing card (cat# MIBA-020–60 mm) and lateral flow cassettes (cat# MICA-200) for test strips were purchased from DCN Diagnostics (Carlsbad, CA). De-identified archived tPSA serum samples (n = 18) were obtained from the biorepository for the Biospecimen and Pathology Core of the Weill Cornell Medicine Specialized Programs of Research Excellence (SPORE) in Prostate Cancer. Commercially purchased human whole blood (Innovative Research, Inc., Novi, MI) samples (n = 6) from female donors was used for spiked whole blood analysis. This article does not contain any studies involving human participants and ethical approval was not required.

### 2.2. Equipment

Equipment used in this study included ultrasonic cleaner (DK Sonic, model DK-300 s), incubated tube rotator (Roto-Therm™ model H2024), centrifuge (Eppendorf 5415D), lateral flow reagent dispenser (Matrix 1600, Kinematic Automation, Inc.), test strip cutting module (Matrix 2360, Kinematic Automation, Inc.) Spectrophotometer (VWR V-1200), IMMULITE 2000 analyzer (Siemens Healthcare Laboratory Diagnostics), and Cube Reader (Chembio Diagnostics GmbH, Berlin, Germany) with custom-made test strip adapter.

### 2.3. Preparation of gold nanoshells (AuNS<sub>h</sub>) conjugated with anti-PSA antibody

Fig. 1A shows a schematic of the various steps involved in conjugation of anti-PSA antibody to AuNS<sub>h</sub>. To prepare AuNS<sub>h</sub> conjugated with anti-PSA antibody, 1 mL of the AuNS<sub>h</sub> were

first transferred to a microcentrifuge tube and brought to room temperature. AuNS<sub>h</sub> particles were briefly vortexed and sonicated for 30 s in full-wave mode (40KHz) to fully disperse the particles. A freshly prepared mixture of 8ul of EDC at 10 mg/ml concentration and 16ul of sulfo-NHS at 10 mg/ml concentrations in DI water was added to the microcentrifuge with NS. The mixture in the microcentrifuge was briefly vortexed and sonicated for 30 s and then incubated for 30 min on the tube rotator in mix mode at 25 °C. After incubation the AuNS<sub>h</sub> mixture was centrifuged at 2000 RCF for 5 min to remove any excess EDS/sulfo-NHS and the supernatant pellet was resuspended in 1 mL of reaction buffer (5 mM potassium phosphate, 0.5% 20 K PEG at pH 7.4). The resuspended particles were briefly vortexed and sonicated for 30 s. The wash step was repeated by centrifuging the AuNS<sub>h</sub> mixture at 2000 RCF and the supernatant pellet was resuspended in 1 mL of reaction buffer. The resuspended particles were briefly vortexed and sonicated for 30 s. After the second wash step, 30µg of anti-PSA detection antibody in MES buffer at pH 6.0 was added to the AuNS<sub>h</sub> mixture and allowed to incubate for 1 h on the tube rotator in mix mode at 25 °C. After incubation, 10 µL of 50% hydroxylamine quencher was added to the AuNS<sub>h</sub> mixture to deactivate any remaining active NHS-esters. The AuNS<sub>h</sub> mixture was briefly vortexed and incubated at room temperature for 10 min on the tube rotator in mix mode at 25 °C. The AuNS<sub>h</sub> mixture was washed and resuspended twice by centrifuging at 2000 RCF for 5 min, and supernatant resuspended in 1 mL of reaction buffer, followed by brief vertexing and sonication for 30 s. The twice-washed AuNS<sub>h</sub> mixture was centrifuged at 2000 RCF for 5 min and the pellet was resuspended in 1 mL of conjugate diluent (0.5X PBS, 0.5% BSA, 0.5% casein, 1% Tween-20, 0.05% sodium azide, pH 8). The prepared AuNS<sub>h</sub>-anti-PSA-antibody conjugate was stored at 4 °C until further use.

#### 2.4. Preparation of gold nanosphere (AuNS<sub>p</sub>) conjugated with anti-PSA antibody

Fig. 1B shows a schematic of the various steps involved in conjugation of anti-PSA antibody to AuNS<sub>p</sub>. To prepare gold nanosphere (AuNS<sub>p</sub>) conjugated with anti-PSA antibody, all the reagents of the conjugation kit were first brought to room temperature. Stock anti-PSA antibody was diluted to 0.1 mg/ml with the antibody diluent provided in the kit. Diluted antibody (12 µL) was then added to 42 µL of the reaction buffer provided in the kit and 45 µL of this mixture was added to the lyophilized AuNS<sub>p</sub> vial in the kit. The mixture in the vial was gently pipetted to ensure mixing and resuspension of the gold nanospheres and antibody solution and allowed to incubate at room temperature for 15 min. After 15 min of incubation, 5 µL of quencher provided in the kit was added to the vial and the reaction was left at room temperature for 5 min to yield 50 µL of AuNS<sub>p</sub>-anti-PSA-antibody conjugate at 20 OD. To remove any unbound antibodies, ten times the volume of the 1:10 diluted quencher was added to the conjugate in the vial, followed by a centrifugation step at 9,000g for 10 min. The supernatant after centrifugation was carefully pipetted to be discarded and the AuNS<sub>p</sub>-anti-PSA-antibody conjugate pellet was resuspended in 1:10 diluted quencher in DI water for storage at 4 °C until further use.

#### 2.5. Lateral flow test strip assembly

Fig. 2 shows a schematic of the various components of the assembled lateral flow assay test strip. The test and control line antibodies were dispensed on the nitrocellulose membrane using the lateral flow reagent dispenser (flow rate 10 µL/cm) to dispense monoclonal anti-

PSA capture antibody (1 mg/mL in PBS buffer) on the test line and anti-mouse IgG (1.8 mg/mL in PBS buffer) on the control line. The nitrocellulose membranes were subsequently dried for two hours at 37 °C and stored in an airtight box along with silica gel desiccants at room temperature. To prepare the conjugate pads, the stock AuNS<sub>h</sub>-anti-PSA-antibody conjugate solution was first diluted to 3 OD with gold conjugate stabilizer. The conjugate membrane was cut to 10 mm × 250 mm strip and was soaked in the diluted conjugate for one minute, followed by oven drying at 37 °C for 12 h. The sample pad membrane was soaked in blocking buffer for 1 h at room temperature with shaking followed by a wash step in wash buffer (1X PBS with 0.05% Tween-20) for 15 min. The blocked sample pad membrane was dried in the oven at 37 °C for 12 h. The dried sample pad membrane was then cut to 10 mm × 250 mm strips. The nitrocellulose membrane was attached to the backing card, followed by attaching the conjugate pad, sample pad, and the waste pad, all with 2 mm overlap. In test strips used for whole blood assay, sample pad was replaced by blood separation membrane and a masking tape was applied to partially cover the conjugate pad and nitrocellulose membrane to ensure the pads remain in place. The assembled card was cut into individual strips of 5 mm width using the test strip cutting module. A similar approach was followed for preparation of AuNS<sub>p</sub>-labeled lateral flow assay strips with conjugate pad containing 0.3 OD of the AuNS<sub>p</sub>-anti-PSA-antibody. The test strips were individually housed within a test strip cassette and stored at room temperature in a heat-sealed foil pouches with silica gel.

## 2.6. Testing protocol

Fig. 3A shows a schematic of the various steps involved in conducting the point-of-care tPSA testing. Briefly, the user first adds the test sample comprising a mixture of the sample (archived serum or serum-based calibrator) and running buffer (1X PBS with 1% Tween20 and 0.1% sodium azide) to the test strip to initiate capillary flow within the test strip, which causes the AuNS<sub>h</sub>-labeled anti-PSA-antibody conjugates to be released from the conjugate pad. The tPSA antigen in the test sample reacts with the AuNS<sub>h</sub>-anti-PSA-antibody conjugates and flows downstream to further react with the antibodies at the test and control lines. The remaining sample is finally collected in the absorbent pad. The test strip is then inserted into the test strip adapter of the Cube<sup>TM</sup> reader to record the test to control line intensity (TC) ratio values.

## 2.7. Cube<sup>TM</sup> reader configuration and data processing

Fig. 3B shows the main data processing steps within the Cube<sup>TM</sup> reader. The Cube<sup>TM</sup> configuration software was programmed to define the relative location, search width and width of the test and control lines on the test strip. A white background image of the nitrocellulose membrane on an unused test strip was captured and saved as reference image for background subtraction. The intensities of the test and control line are calculated based on the area (blue shade) and the test to control line intensity (TC) ratio is calculated. Cube<sup>TM</sup> can be programmed to store an experimentally determined calibration function that correlates TC ratios and tPSA concentration. Cube<sup>TM</sup> displays the tPSA concentration based on the pre-stored calibration function. Cube<sup>TM</sup> offers an internal memory to safely store the measurement results that can be exported to other platforms as required. The small form

factor ( $1.6 \times 1.6 \times 1.6$  in), lightweight (~1.4 oz), and battery-operated features of the Cube™ makes it a highly portable solution for point of care PCa screening.

## 2.8. Data analysis

Statistical analysis of data was done with Microsoft Excel for Microsoft 365 MSO (Microsoft, Redmond WA). In experiments for determining calibration curves with tPSA calibrator, power regression model was used to test if average TC ratios measured from point-of-care testing significantly predicted tPSA concentrations of the calibrator samples. To determine the degree of correlation between serum tPSA concentrations predicted by point-of-care approach and tPSA concentrations determined by gold standard IMMULITE method, simple linear regression analysis was done. In addition, intraclass correlation coefficient (ICC) (Koo and Li, 2016) was calculated to determine both degree of correlation and agreement between point-of-care and IMMULITE tPSA measurements with serum samples.

## 3. Results

### 3.1. Comparison of test line intensities between AuNS<sub>h</sub> and AuNS<sub>p</sub>-labeled test strips

The test line intensities of AuNS<sub>h</sub> and AuNS<sub>p</sub>-labeled conjugate versions of the test strips were compared by testing with various concentrations of the Access Hybritech total PSA calibrator. Testing involved adding 20 μL of the tPSA calibrator and 60 μL of running buffer to the test strips. The test was run in triplicates for both AuNS<sub>h</sub> and AuNS<sub>p</sub>-labeled version of the test strips for each calibrator concentration and their test line intensities were recorded with Cube™ after 20 min of reaction time. Fig. 4A shows representative images of the colorimetric changes in test and control lines on both AuNS<sub>h</sub> and AuNS<sub>p</sub>-labeled test strip pairs for each tPSA concentration tested. Fig. 4B shows a grouped bar chart, where the x-axis indicates average test line intensities measured with Cube™ reader in AuNS<sub>h</sub> and AuNS<sub>p</sub>-labeled test strip pairs grouped by each tPSA calibrator concentration tested (shown on y-axis). Error bars represent standard deviations of test line intensity measurements with Cube™ from samples assayed in triplicate. The test line intensity with gold AuNS<sub>p</sub> label was not visible to the naked eye at a concentration of 0.5 ng/mL and no measurable signal was detected with Cube™. The test line with gold AuNS<sub>p</sub> at 2.5 ng/mL was also not visible to the naked eye but signal was detected by the Cube™ reader. Unlike AuNS<sub>p</sub>-labeled version of the test strip, test line was visible to the naked eye with AuNS<sub>h</sub>-labeled test strip and a signal was also recorded with the Cube™ for the entire range of PSA calibrator concentrations tested. As can be observed from Fig. 4B, for all tPSA concentrations tested, test line intensity with the AuNS<sub>h</sub>-labeled test strip was higher than the AuNS<sub>p</sub>-labeled test strips. Based on these results, AuNS<sub>h</sub>-labeled test strip was selected over the AuNS<sub>p</sub>-labeled version for further testing.

### 3.2. Immunoreaction kinetics analysis with ACCESS Hybritech tPSA calibrator

The kinetic curve of detection antibody (AuNS<sub>h</sub>-anti-PSA-antibody) and antigen (tPSA captured on test line) interaction was determined to decide the optimal time at which measurements can be made with Cube™ reader for tPSA testing. A 20 μL sample of the calibrator was added to the test strip along with 60 μL of the running buffer. Test strips

were run in triplicates for each concentration available in the calibrator kit. The test strip was inserted into the test strip adapter of the Cube™ portable test strip reader. The signal intensities of the T line and C line were recorded on Cube™ every 30 sec for 30 min duration after addition of sample. As shown in Fig. 5, the kinetic curves were analyzed by plotting the signal intensity of T line measured by the Cube™ against time. It can be observed that there is measurable difference in average test line intensity for concentrations as early as within 5 to 10 min for tPSA concentrations 10 ng/mL and above. However, at concentrations of 2.5 ng/mL and lower, the difference in average test line intensities is only measurable between 15 and 20 min. Therefore, all measurements with Cube™ were made at 20 min to obtain a measurable difference in test line intensities for the concentration ranging from 0.5 to 150 ng/mL.

### 3.3. Calibration curve with ACCESS Hybritech tPSA calibrator

The contents of the calibrator vials were mixed gently by inverting before use. AuNS<sub>h</sub>-labeled test strips were run in triplicates for each concentration available in the calibrator kit. A 20 µL sample of the calibrator was added to the AuNS<sub>h</sub>-labeled test strip along with 60 µL of the running buffer. After 20 min of reaction time, the test strip was inserted into the test strip adapter of the Cube™ reader to record the signal as TC ratio. Hybritech tPSA Calibrators provides two options for calibration - Hybritech calibration or WHO calibration. For Hybritech calibration, the analyte in the Access Hybritech PSA Calibrators is traceable to the manufacturer's working calibrator with the Traceability process based on EN ISO 17511. For WHO calibration, the analyte in the calibrators is traceable by comparison with a set of primary reference calibrators standardized to the WHO First International Standard (1st IS) for PSA (WHO 96/670). Testing with calibrator is useful to determine whether the selected antibodies and test strip configuration are suitable to achieve the detection range. Fig. 6 shows a scatterplot and power model fitted trendline for a set of 5 calibrator concentrations tested with AuNS<sub>h</sub>-labeled test strips, with tPSA calibrator concentrations shown on x-axis and average TC ratios measured with Cube™ shown on the y-axis. Error bars represent standard deviations of measured TC ratio results from samples assayed in triplicate. The fitted power model was  $[TC \text{ ratio}] = 0.0229 * [tPSA, \text{ calibrator}]^{0.7991}$ , where [tPSA, calibrator] and [TC ratio] represent tPSA calibrator concentration (ng/mL) and measured average TC ratio with Cube™, respectively. The overall regression was statistically significant with  $R^2 = 0.9938$ , 95% CI [0.9210, 0.6771],  $F(1, 3) = 434.97$ ,  $p < .0001$ . Test results with tPSA calibrators confirmed that the selected antibody pair in a sandwich assay format and the test strip configuration provided the detection range covering tPSA calibrator concentrations in the range 0.5–150 ng/mL

### 3.4. Calibration curve with archived serum samples

The performance of the AuNS<sub>h</sub>-labeled tPSA test strips was further evaluated with archived human serum samples (n = 18). Gold standard reference quantification for tPSA was done by testing with Siemens IMMULITE 2000 automated immunoassay system. For each sample assayed in triplicate, testing with the point of care approach involved adding 20 µL of the serum sample and 60 µL of running buffer to the test strips. Representative images of the colorimetric changes of the test and control lines on the test strip after test completion at various known concentrations of serum samples shown below each test

strip image, in increasing order from left to right, are presented in Fig. 7A. As expected for a sandwich assay format, it can be observed from the test strip images in Fig. 7A that the intensity of test line also increases as the concentration of tPSA increases, with no measurable test line for negative control sample. The test results from test strips were included in the analysis if at least one of the test strips developed completely with both control line and test line detected by the Cube™ reader. We selected TC ratios data for a subset of the serum samples against the corresponding reference method (IMMULITE) results to obtain an initial calibration curve. This calibration curve was then applied to predict the tPSA concentrations of the remaining samples tested with our point-of-care screening test approach. Fig. 7B shows a scatterplot and the regression line for a set of 13 samples, with predicted tPSA concentrations from point-of-care approach on y-axis and tPSA concentrations quantified by IMMULITE method on the x-axis. Error bars represent standard deviations of predicted tPSA concentration results from tests run in triplicate. Simple linear regression was used to test if the point-of-care approach significantly predicted tPSA concentrations quantified by gold standard IMMULITE method. The fitted regression model was  $[tPSA, POC] = 1.2354*[tPSA, IMMULITE] + 1.4737$ , where  $[tPSA, POC]$  and  $[tPSA, IMMULITE]$  represent predicted tPSA concentration (ng/mL) from point-of-care approach and measured tPSA concentration (ng/mL) by IMMULITE, respectively. The overall regression was statistically significant with  $R^2 = 0.902$ , 95% CI [0.9488, 1.521],  $F(1, 10) = 92.311$ ,  $p < .0001$ . Intraclass correlation (Koo and Li, 2016) (ICC) test with one-way random, average score model was calculated to assess agreement between averaged measurement of three readings for each concentration tested with point-of-care approach and IMMULITE testing. Based on the 95% confident interval of the ICC estimate, values less than 0.5, between 0.5 and 0.75, between 0.75 and 0.9, and greater than 0.90 are indicative of poor, moderate, good, and excellent reliability, respectively (Koo and Li, 2016). Calculated ICC was found to be excellent with calculated ICC (1, 3) value of 0.916 (95% CI, 0.707–0.977).

### 3.5. Testing with spiked whole blood and extracted serum

Commercially purchased human whole blood from female donors ( $n = 6$ ) was used for the whole blood analysis. Studies show that PSA is present at very low concentrations in female serum and with conventional PSA assays with a detection limit of 0.1–0.01 ng/mL, PSA is detectable in less than 10% of female sera (Melegos et al., 1997). The focus of this analysis is to determine if the AuNS<sub>11</sub>-labeled test strip is compatible with whole blood matrix. Refrigerated whole blood samples were first brought to room temperature. It was observed that no measurable TC ratio signals were recorded with Cube™ reader when whole blood samples were used as is without any spiking with tPSA. Whole blood samples were spiked with tPSA from the commercial tPSA calibration kit with concentration ranging 2.5–75 ng/mL. Testing involved adding 20  $\mu$ L spiked whole blood sample with 80  $\mu$ L of the running buffer. Test samples were assayed in triplicates for each spiked whole blood concentration tested. Serum samples from the spiked whole blood samples were extracted by centrifugation at 1500g for 20 min. Extracted serum samples were tested by adding 20  $\mu$ L of serum with 80  $\mu$ L of the running buffer and test strips were run in triplicates for each extracted serum sample. Representative images of the colorimetric changes of the test and control lines on the test strip after test completion at various known concentrations

of spiked whole blood samples (top row) and extracted serum samples (bottom row) are presented in Fig. 8A. Fig. 8B shows a grouped bar chart, where the x-axis indicates spiked tPSA concentrations and the y-axis indicates average test line intensities measured with Cube™ reader in for spiked whole blood and extracted serum pairs for each spiked tPSA concentration tested. Red dashed and blue dotted lines represent third order polynomial model trendline fitted for spiked whole blood and extracted serum data, respectively. The fitted regression model for spiked whole blood data ( $R^2 = 0.9813$ ) was [TC ratio, spiked whole blood] =  $-0.0003 * [\text{tPSA, spiked}]^3 + 0.0116 * [\text{tPSA, spiked}]^2 - 0.027 * [\text{tPSA, spiked}] + 0.0598$ , where [tPSA, spiked] and [TC ratio, spiked whole blood] represent spiked tPSA calibrator concentration (ng/mL) and measured average TC ratio with Cube™ for spiked whole blood samples, respectively. The fitted regression model for extracted serum data ( $R^2 = 0.9821$ ) was [TC ratio, extracted serum] =  $-0.0004 * [\text{tPSA, spiked}]^3 + 0.0151 * [\text{tPSA, spiked}]^2 - 0.0502 * [\text{tPSA, spiked}] + 0.0853$ , where [tPSA, spiked] and [TC ratio, extracted serum] represent spiked tPSA calibrator concentration (ng/mL) and measured average TC ratio with Cube™ for extracted serum samples, respectively. It can be observed that the measured TC ratio values increased with increasing tPSA concentration for both spiked whole blood and extracted serum sample pairs, as expected for a sandwich assay format implemented in the test strip design. It can also be observed from Fig. 8B, that the average TC ratio values with spiked whole blood was lower than the corresponding extracted serum for the spiked whole blood and extracted serum pairs tested, especially at tPSA concentrations ranging 12.5–75 ng/mL. Differences in whole blood and serum sample viscosities leads to different wicking speeds and thus different flow rates through the test strip membrane. And viscosity dependent flow rates due to various samples viscosities causes varying incubation times for the molecules at the binding sites. The consequence is viscosity bias in the signal intensities and thus over- or underestimations of the analyte concentrations (Kainz et al., 2021). The use of running buffer helps in reducing the viscosity effects of various sample types. Besides viscosity effects, test line intensity with samples such as whole blood is reduced in a sandwich assay format when compared to serum due to possible interference from matrix components of whole blood, referred to as matrix effect (Wood, 1991). For whole blood and serum samples, differences in background color of the nitrocellulose membrane can be observed when hemolysis occurs, and this background color can interfere with measurement of colorimetric changes on the test line by the test strip reader. Hemolysis can be reduced by proper choice of blood separation membrane and running buffer. In our previous work, we have reported (Lu et al., 2018) development of technology referred to “high yield passive erythrocyte removal” (HYPER), which utilizes capillary forces in a unique cross-flow filtration for the separation of whole blood with performance comparable to centrifuge. Also, use of freshly collected blood that is used immediately on the test strip is less prone to hemolysis with more uniform flow when compared to stored whole blood.

#### 4. Discussion

In this study, we demonstrated a proof of concept for a sandwich-type lateral flow immunoassay based on a AuNS<sub>h</sub> label with a highly portable reader for the quantification of tPSA concentrations in human serum and spiked whole blood samples.

#### 4.1. Study strengths and limitations

The number of test samples used in our current study was limited as the focus of this study was to develop a proof of concept and test the prototype with a range of tPSA concentrations with archived serum and spiked whole blood samples, while keeping the initial development costs to a minimum. In future studies, we plan to optimize the performance of the tPSA point-of-care technology using freshly collected whole blood by fingerprick in human validation studies among greater number of participants, to improve the calibration curve and perform a comprehensive evaluation of diagnostic performance. De-identified serum samples with a wide range of known tPSA concentrations quantified by gold standard IMMULITE method were used for validation of the point-of-care method in the lab. The use of known range of serum tPSA concentrations introduces sampling bias and can be tested in future work by blinding the results from gold standard method and point-of-care method. Source of Interference from sample matrix components such as the various anticoagulants used during whole blood collection, loss of analytes during serum isolation process can introduce measurement bias and further studies with different types of anticoagulants can be useful in determining the sample compatibility with the developed assay. Test strips were manually assembled and measurement bias due to differences in various batches of test strips can be reduced in future work by contract manufacturing test strips at a test strip manufacturing facility after optimizing test strip design through more rigorous testing. Patient information such as age and ethnicity were not considered in this study as the focus was to perform preliminary validation and analytical performance characterization of the lateral flow immunoassay in terms of detection range, selection of antibodies, selection of various buffers, test strip membrane components and comparison with results from gold standard laboratory method.

#### 4.2. Comparison of AuNS<sub>h</sub> and AuNS<sub>p</sub>-labeled test strips

We compared the results of tPSA quantification with AuNS<sub>h</sub>-labeled test strips against the widely used 40 nm gold AuNS<sub>p</sub> label. We demonstrated that the AuNS<sub>h</sub>-labeled test strips provided a higher intensity of colorimetric signal for the test line over the entire range of tPSA concentrations tested. It was also observed that at a lower concentration of 0.5 ng/ml, AuNS<sub>h</sub> test strips produced a readable signal with Cube™ whereas no measurable signal could be recorded with AuNS<sub>p</sub>-labeled test strips. The percentage increase in test line colorimetric signal intensity with AuNS<sub>h</sub>-labeled test strips when compared to AuNS<sub>p</sub> ranged from 64.3% (at tPSA concentration 2.5 ng/ml) to 188.3% (at tPSA concentration 10 ng/ml). AuNS<sub>h</sub> as a label provides the advantage of detecting lower concentrations of tPSA, with 5 times lower detection limit than AuNS<sub>p</sub>, without the need for any additional signal amplification steps such as silver enhancement or use of fluorescent labels that require specialized test strip readers with additional optics that are expensive.

#### 4.3. Immunoreaction kinetics analysis

The time instant at which the test strip signal is measured with the Cube™ reader is critical since the test line colorimetric signal intensity and the difference in test line intensities at various concentrations of tPSA tested is time dependent. At lower concentrations in the range 0.5–2.5 ng/mL, the difference in test line intensities between 0.5 and 2.5 ng/mL was

measurable with the Cube™ as early as 10 min, with the measured signal intensity at 2.5 ng/mL twice that of 0.5 ng/mL. At 20 min, the test line intensity for 2.5 ng/mL is 3.7 times higher than 0.5 ng/mL. At lower concentration ranges, close to the tPSA cutoff value of 4 ng/mL, the test line intensity tends to have less fluctuations as time progresses. The test strip readout time was chosen as 20 min to achieve repeatable results, to account for and minimize the signal variations expected between test strips of different batches produced. In future, the optimal readout time required can be reduced to as low as 10 min, by further optimizing the test strip preparation steps and preferably with test strips assembled by automated test strip manufacturing process.

#### 4.4. Testing with various sample types

We determined calibration curves for the point-of-care tPSA assay with commercially available ACCESS Hybritech PSA calibrators and archived serum samples with tPSA quantified on IMMULITE analyzer. The detection range demonstrated with the calibrator kit was 0.5 to 150 ng/mL. The point-of-care tPSA assay was successfully applied to quantify tPSA concentrations in archived serum samples with concentrations ranging from 2.2 to 65 ng/mL. The performance of tPSA quantification with our point-of-care screening technology was comparable to performance of the laboratory standard IMMULITE for serum samples. On preliminary testing with archived serum samples and comparison with IMMULITE, a correlation of 0.95 ( $p < .0001$ ) was observed.

We also tested whole blood samples spiked with tPSA calibrator to confirm the compatibility of the test strips with possible interference due to whole blood matrix components. Extracted serum from spiked whole blood samples was tested to compare the measured signal intensities. It observed that the measured TC ratio values increased with increasing tPSA concentration for both spiked whole blood and extracted serum sample pairs, as expected for a sandwich assay format implemented in the test strip design. And overall, the signal intensity for extracted serum was greater than whole blood samples and is expected due to viscosity effects and possible interference from matrix components of whole blood.

#### 4.5. Role of tPSA

Studies have estimated that elevated tPSA concentrations may precede clinical manifestations of prostate cancer by 5 to 10 or more years (Gann et al., 1995) (Draisma et al., 2003). However, elevated tPSA may also be observed without PCa in men with ongoing benign conditions such as benign prostatic hyperplasia or transient conditions such as prostatitis. The most accepted serum tPSA cut-off for predicting PCa is 4.0 ng/mL. However, in certain conditions such as where the patient is taking a 5-alpha reductase inhibitor (ARI), a correction factor is to be applied to tPSA result for accurate interpretation, since ARIs are known to lower total PSA results. Some experts prefer age cohort-specific reference ranges for tPSA, instead of relying on a single cutoff value for all age groups. Serum tPSA levels generally are known to increase with age, partly because of the likelihood of benign enlarged prostate in older men leading to producing larger amounts of PSA. However, currently sufficient data is not available to support precise age cohort-specific reference values. Besides age, men from different ethnic and racial groups

without PCa have different average tPSA concentrations. Studies have shown that black men without prostate cancer tend to have higher PSA values than white men without prostate cancer. It has been proposed that the definition of a “normal” PSA should vary by race using race-specific reference ranges (Morgan et al., 1996). However, in clinical practice race-specific reference ranges for tPSA are not typically applied currently for PCa. Another application of tPSA screening test is for patients who are undergoing treatment for PCa. These patients require frequent serum tPSA quantification and the availability of a point-of-care screening test that can be performed at home will play a significant role in improving patient compliance.

## 5. Conclusions

Most tPSA testing currently depends on dedicated centralized laboratories using large, automated analyzers, with increasing turnaround times causing delays in patient care, and increased administration and medical costs. The 150 nm diameter gold nanoshell label reported in this study can be applied as an alternative to the widely used 40 nm gold nanospheres for various lateral flow assays to increase the colorimetric signal intensities without additional signal amplification steps and achieve lower detection limits. The application of point-of-care approach for tPSA quantification has the capability to quantify tPSA from a drop of serum or whole blood within a few minutes. Oncologists and urologists in clinical practice worldwide often depend on a serum PSA quantification test to direct patient care for both initial PCa screening and for post-treatment monitoring of patients. More often an additional visit by the patient is needed after obtaining the test results from the diagnostic lab with a long turnaround time. Our point-of-care test has the potential to significantly simplify and accelerate patient care by enabling serum tPSA test while the patient is still in the doctors’ office for the consultation. This near-patient screening with results available within 20 min would enable physicians to quickly decide if additional diagnostic testing with a multiparametric MRI or prostate biopsy is required for the patient.

## Acknowledgements

The authors would like to thank the following: Victoria Simon, Cornell University Human Nutritional Chemistry Service Laboratory, for conducting reference tests on IMMULITE; Elizabeth J. Robinson from Ahlstrom-Munksjö for providing samples of lateral flow test pads used in this study; the biorepository at Weill Cornell Medicine (WCM) through the Specialized Programs of Research Excellence (SPoRE) in prostate cancer for providing archived serum samples. Figs. 1, 2, 3 and graphical abstract were created with [BioRender.com](https://BioRender.com)

## Funding

The research reported in this publication was partly supported by the National Institute of Biomedical Imaging and Bioengineering of the National Institutes of Health (NIH) under award number R01EB021331 and the National Cancer Institute/NIH award number P50CA211024. The content is solely the responsibility of the authors and does not necessarily represent the official views of the National Institutes of Health.

## Abbreviations:

<b>PCa</b>	prostate cancer
<b>PSA</b>	prostate-specific antigen
<b>tPSA</b>	total PSA

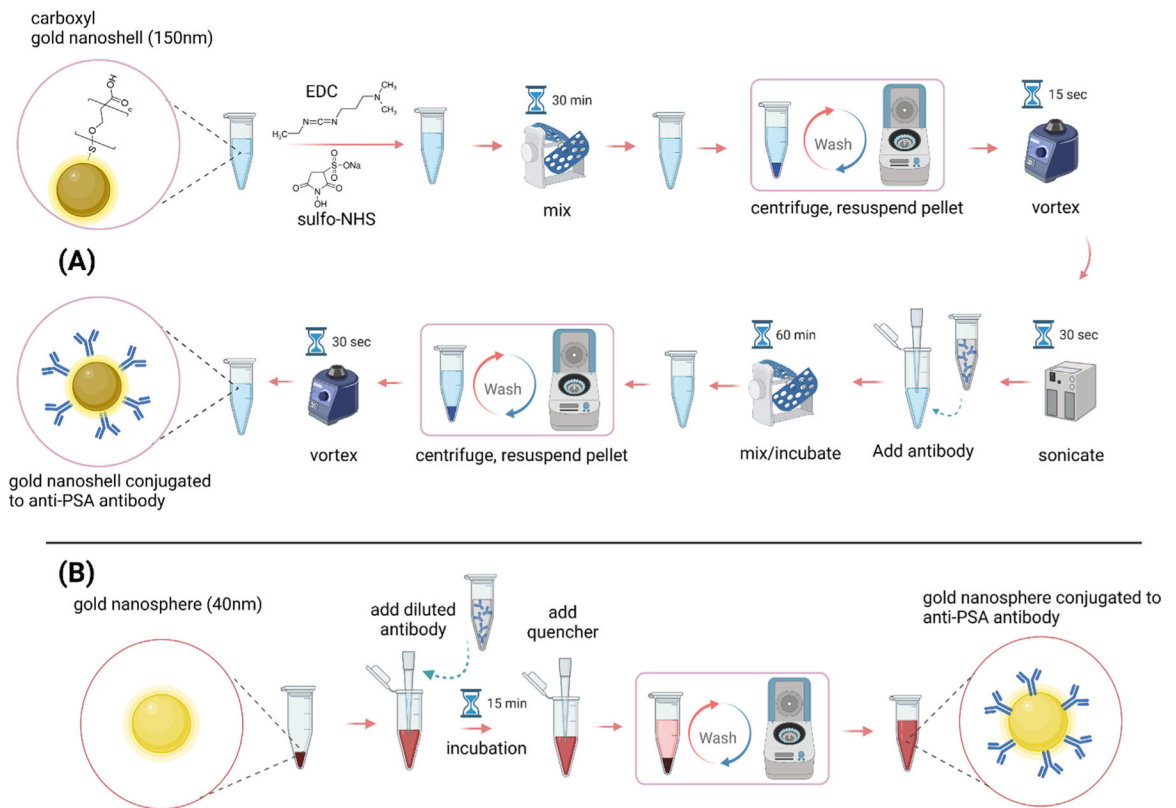
<b>POCT</b>	point-of-care testing
<b>AuNS<sub>h</sub></b>	gold nanoshells
<b>AuNP<sub>h</sub></b>	gold nanospheres
<b>AA</b>	African American
<b>LFIA</b>	lateral flow immunoassay
<b>TC</b>	test-to-control-line intensity

## References

- Andreeva IP, Grigorenko VG, Egorov AM, Osipov AP, 2016. Quantitative lateral flow immunoassay for total prostate specific antigen in serum. *Anal. Lett* 49 (4), 579–588. 10.1080/00032719.2015.1075130.
- Barbosa AI, Castanheira AP, Edwards AD, Reis NM, 2014. A lab-in-a-briefcase for rapid prostate specific antigen (PSA) screening from whole blood. *Lab Chip* 14 (16), 2918–2928. 10.1039/C4LC00464G. [PubMed: 24989886]
- Brawley OW, 2012. Trends in prostate cancer in the United States. *J. Natl. Cancer Instit.. Monographs* 2012 (45), 152–156. 10.1093/jncimonographs/lgs035.
- Chang H, Kang H, Ko E, Jun B-H, Lee H-Y, Lee Y-S, Jeong DH, 2016. PSA detection with femtomolar sensitivity and a broad dynamic range using SERS nanoprobe and an area-scanning method. *ACS Sens.* 1 (6), 645–649. 10.1021/acssensors.6b00053.10.1021/acssensors.6b00053.s001.
- Chornokur G, Arya SK, Phelan C, Tanner R, Bhansali S, 2011. Impedance-based miniaturized biosensor for ultrasensitive and fast prostate-specific antigen detection. *J. Sens* 2011, 1–7. 10.1155/2011/983752.
- Dong Y-X, Cao J-T, Liu Y-M, Ma S-H, 2017. A novel immunosensing platform for highly sensitive prostate specific antigen detection based on dual-quenching of photocurrent from CdSe sensitized TiO<sub>2</sub> electrode by gold nanoparticles decorated polydopamine nanospheres. *Biosens. Bioelectron* 91, 246–252. 10.1016/j.bios.2016.12.043. [PubMed: 28013019]
- Draisma G, Boer R, Otto SJ, van der Crujisen IW, Damhuis RA, Schröder FH, de Koning HJ, 2003. Lead times and overdetection due to prostate-specific antigen screening: estimates from the European Randomized Study of Screening for Prostate Cancer. *J. Natl. Cancer Instit* 95 (12), 868–878. 10.1093/jnci/95.12.868.
- Ertürk G, Hedström M, Tümer MA, Denizli A, Mattiasson B, 2015. Real-time prostate-specific antigen detection with prostate-specific antigen imprinted capacitive biosensors. *Anal. Chim. Acta* 891, 120–129. 10.1016/j.aca.2015.07.055. [PubMed: 26388370]
- Ertürk G, Özen H, Tümer MA, Mattiasson B, Denizli A, 2016. Microcontact imprinting based surface plasmon resonance (SPR) biosensor for real-time and ultrasensitive detection of prostate specific antigen (PSA) from clinical samples. *Sens. Actuators, B* 224, 823–832. 10.1016/j.snb.2015.10.093.
- Etzioni R, Tsodikov A, Mariotto A, Szabo A, Falcon S, Wegelin J, diTommaso D, Karnofski K, Gulati R, Penson DF, Feuer E, 2008. Quantifying the role of PSA screening in the US prostate cancer mortality decline. *Cancer Causes Control* 19 (2), 175–181. 10.1007/s10552-007-9083-8. [PubMed: 18027095]
- Foysal KH, Seo SE, Kim MJ, Kwon OS, Chong JW, 2019. Analyte quantity detection from lateral flow assay using a smartphone. *Sensors (Basel, Switzerland)* 19 (21), 4812. 10.3390/s19214812.
- Gann PH, Hennekens CH, Stampfer MJ, 1995. A prospective evaluation of plasma prostate-specific antigen for detection of prostatic cancer. *JAMA* 273 (4), 289–294. [PubMed: 7529341]
- Gutiérrez-Zúñiga GG, Hernández-López JL, 2014. Sandwich-type ELISA Impedimetric Immunosensor for Early Detection of Prostate-specific Antigen (PSA) in Human Serum. *Procedia Chem.* 12, 47–54. 10.1016/j.proche.2014.12.040.

- Hewitt T, Killinger KA, Hiller S, Boura JA, Lutz M, 2018. Exploring racial differences surrounding prostate cancer screening: beliefs and attitudes in community dwelling men attending an urban men's health event. *Am. J. Men's Health* 12 (6), 1929–1936. 10.1177/1557988318784838. [PubMed: 29952245]
- Juntunen E, Myyryläinen T, Salminen T, Soukka T, Pettersson K, 2012. Performance of fluorescent Europium(III) nanoparticles and colloidal gold reporters in lateral flow bioaffinity assay. *Anal. Biochem* 428 (1), 31–38. 10.1016/j.ab.2012.06.005. [PubMed: 22705171]
- Kainz DM, Breiner BJ, Früh SM, Hutzenlaub T, Zengerle R, Paust N, 2021. Eliminating viscosity bias in lateral flow tests. *Microsyst. Nanoeng* 7 (1), 72. 10.1038/s41378-021-00296-5. [PubMed: 34567784]
- Kavosi B, Salimi A, Hallaj R, Amani K, 2014. A highly sensitive prostate-specific antigen immunosensor based on gold nanoparticles/PAMAM dendrimer loaded on MWCNTS/chitosan/ionic liquid nanocomposite. *Biosens. Bioelectron* 52, 20–28. 10.1016/j.bios.2013.08.012. [PubMed: 24016535]
- Kensler KH, Pernar CH, Mahal BA, Nguyen PL, Trinh QD, Kibel AS, Rebbeck TR, 2021. Racial and ethnic variation in PSA testing and prostate cancer incidence following the 2012 USPSTF recommendation. *J. Natl. Cancer Inst* 113 (6), 719–726. 10.1093/jnci/djaa171.
- Kong R-M, Ding L, Wang Z, You J, Qu F, 2015. A novel aptamer-functionalized MoS<sub>2</sub> nanosheet fluorescent biosensor for sensitive detection of prostate specific antigen. *Anal. Bioanal. Chem* 407 (2), 369–377. 10.1007/s00216-014-8267-9. [PubMed: 25366976]
- Koo TK, Li MY, 2016. A guideline of selecting and reporting intraclass correlation coefficients for reliability research. *J. Chiropractic Med* 15 (2), 155–163. 10.1016/j.jcm.2016.02.012.
- Kost GJ, 1995. Guidelines for point-of-care testing. Improving patient outcomes. *Am. J. Clin. Pathol* 104 (4 Suppl 1), S111–127. [PubMed: 7484942]
- Lee S, O'Dell D, Hohenstein J, Colt S, Mehta S, Erickson D, 2016. NutriPhone: a mobile platform for low-cost point-of-care quantification of vitamin B12 concentrations. *Sci. Rep* 6 (1), 28237. 10.1038/srep28237. [PubMed: 27301282]
- Li X, Li W, Yang Q, Gong X, Guo W, Dong C, Liu J, Xuan L, Chang J, 2014. Rapid and quantitative detection of prostate specific antigen with a quantum dot nanobeads-based immunochromatography test strip. *ACS Appl. Mater. Interfaces* 6 (9), 6406–6414. 10.1021/am5012782. [PubMed: 24761826]
- Lu Z, Rey E, Vemulapati S, Srinivasan B, Mehta S, Erickson D, 2018. High-yield paper-based quantitative blood separation system. *Lab Chip* 18 (24), 3865–3871. 10.1039/C8LC00717A. [PubMed: 30444230]
- Melegos DN, Yu H, Ashok M, Wang C, Stanczyk F, Diamandis EP, 1997. Prostate-specific antigen in female serum, a potential new marker of androgen excess. *J. Clin. Endocrinol. Metabolism* 82 (3), 777–780. 10.1210/jcem.82.3.3792.
- Miller DB, Markt SC, Nguyen CT, Coleman OC, 2021. Prostate cancer screening and young black men: can early communication avoid later health disparities? *J. Cancer Educ* 1–6. 10.1007/s13187-021-01984-6.
- Morgan TO, Jacobsen SJ, McCarthy WF, Jacobson DJ, McLeod DG, Moul JW, 1996. Age-specific reference ranges for serum prostate-specific antigen in black men. *N Engl. J. Med* 335 (5), 304–310. 10.1056/nejm199608013350502. [PubMed: 8663870]
- Nanocomposix, I., 2021. Gold Nanoshells Retrieved from <https://nanocomposix.com/pages/gold-nanoshells>.
- Nelson TJ, Javier-DesLoges J, Deka R, Courtney PT, Nalawade V, Mell L, Murphy J, Parsons JK, Rose BS, 2021. Association of prostate-specific antigen velocity with clinical progression among African American and non-Hispanic white men treated for low-risk prostate cancer with active surveillance. *JAMA Network Open* 4 (5), e219452. 10.1001/jamanetworkopen.2021.9452. [PubMed: 33999164]
- Noone A-M, Cronin KA, Altekruse SF, Howlander N, Lewis DR, Petkov VI, Penberthy L, 2017. Cancer incidence and survival trends by subtype using data from the surveillance epidemiology and end results program, 1992–2013. *Cancer Epidemiol., Biomarkers Prevention: Publ. Am. Assoc.*

- Cancer Res, cosponsored by the American Society of Preventive Oncology 26 (4), 632–641. 10.1158/1055-9965.EPI-16-0520.
- Partin AW, Criley SR, Subong ENP, Zincke H, Walsh PC, Oesterling JE, 1996. Standard versus age-specific prostate specific antigen reference ranges among men with clinically localized prostate cancer: A pathological analysis. *J. Urol* 155 (4), 1336–1339. [PubMed: 8632568]
- Pei H, Zhu S, Yang M, Kong R, Zheng Y, Qu F, 2015. Graphene oxide quantum dots@silver core-shell nanocrystals as turn-on fluorescent nanoprobe for ultrasensitive detection of prostate specific antigen. *Biosens. Bioelectron* 74, 909–914. 10.1016/j.bios.2015.07.056. [PubMed: 26257182]
- Posthuma-Trumpie GA, Korf J, van Amerongen A, 2009. Lateral flow (immuno) assay: its strengths, weaknesses, opportunities and threats. A literature survey. *Anal. Bioanal. Chem* 393 (2), 569–582. 10.1007/s00216-008-2287-2. [PubMed: 18696055]
- Rafique S, Bin W, Bhatti AS, 2015. Electrochemical immunosensor for prostate-specific antigens using a label-free second antibody based on silica nanoparticles and polymer brush. *Bioelectrochemistry* 101, 75–83. 10.1016/j.bioelechem.2014.08.001. [PubMed: 25156671]
- Siegel RL, Miller KD, Fuchs HE, Jemal A, 2021. Cancer Statistics, 2021. *CA Cancer J. Clin* 71 (1), 7–33. 10.3322/caac.v71.110.3322/caac.21654. [PubMed: 33433946]
- So A, Goldenberg L, Gleave ME, 2003. Prostate specific antigen: an updated review. *Can. J. Urol* 10 (6), 2040–2050. [PubMed: 14704108]
- Srinivasan B, O'Dell D, Finkelstein JL, Lee S, Erickson D, Mehta S, 2018. ironPhone: Mobile device-coupled point-of-care diagnostics for assessment of iron status by quantification of serum ferritin. *Biosens. Bioelectron* 99, 115–121. 10.1016/j.bios.2017.07.038. [PubMed: 28750335]
- Sung H, Ferlay J, Siegel RL, Laversanne M, Soerjomataram I, Jemal A, Bray F, 2021. Global cancer statistics 2020: GLOBOCAN estimates of incidence and mortality worldwide for 36 cancers in 185 countries. *CA Cancer J. Clin* 71 (3), 209–249. 10.3322/caac.v71.310.3322/caac.21660. [PubMed: 33538338]
- Uludag Y, Tothill IE, 2012. Cancer biomarker detection in serum samples using surface plasmon resonance and quartz crystal microbalance sensors with nanoparticle signal amplification. *Anal. Chem* 84 (14), 5898–5904. 10.1021/ac300278p. [PubMed: 22681722]
- USPSTF, 2018. Screening for prostate cancer: US preventive services task force recommendation statement. *JAMA* 319(18), 1901–1913. doi:10.1001/jama.2018.3710 [PubMed: 29801017]
- Wang X, Xu R, Sun XU, Wang Y, Ren X, Du B, Wu D, Wei Q, 2017. Using reduced graphene oxide-Ca: CdSe nanocomposite to enhance photoelectrochemical activity of gold nanoparticles functionalized tungsten oxide for highly sensitive prostate specific antigen detection. *Biosens. Bioelectron* 96, 239–245. 10.1016/j.bios.2017.04.052. [PubMed: 28500948]
- Wood WG, 1991. “Matrix effects” in immunoassays. *Scand J. Clin. Lab Invest Suppl.* 51 (sup205), 105–112.
- Woods-Burnham L, Stiel L, Wilson C, Montgomery S, Durán AM, Ruckle HR, Thompson RA, De León M, Casiano CA, 2018. Physician consultations, prostate cancer knowledge, and PSA screening of African American men in the era of shared decision-making. *Am. J. Mens Health* 12 (4), 751–759. 10.1177/1557988318763673. [PubMed: 29658371]
- Wu D, Liu Y, Wang Y, Hu L, Ma H, Wang G, Wei Q, 2016. Label-free electrochemiluminescent immunosensor for detection of prostate specific antigen based on aminated graphene quantum dots and carboxyl graphene quantum dots. *Sci. Rep* 6 (1), 20511. 10.1038/srep20511. [PubMed: 26842737]
- Yan M, Zang D, Ge S, Ge L, Yu J, 2012. A disposable electrochemical immunosensor based on carbon screen-printed electrodes for the detection of prostate specific antigen. *Biosens. Bioelectron* 38 (1), 355–361. 10.1016/j.bios.2012.06.019. [PubMed: 22770827]
- Zhang Y, Liu Y, Li R, Saddam Khan M, Gao P, Zhang Y, Wei Q, 2017. Visible-light driven Photoelectrochemical Immunosensor Based on SnS<sub>2</sub>@mpg-C<sub>3</sub>N<sub>4</sub> for Detection of Prostate Specific Antigen. *Sci. Rep* 7 (1), 4629. 10.1038/s41598-017-04924-x. [PubMed: 28680147]

**Fig. 1.**(A) Conjugation protocol for gold nanoshells (AuNS<sub>h</sub>) to anti-PSA antibody (B)Conjugation protocol for gold nanospheres (AuNS<sub>p</sub>) to anti-PSA antibody. Created with [BioRender.com](https://www.biorender.com).

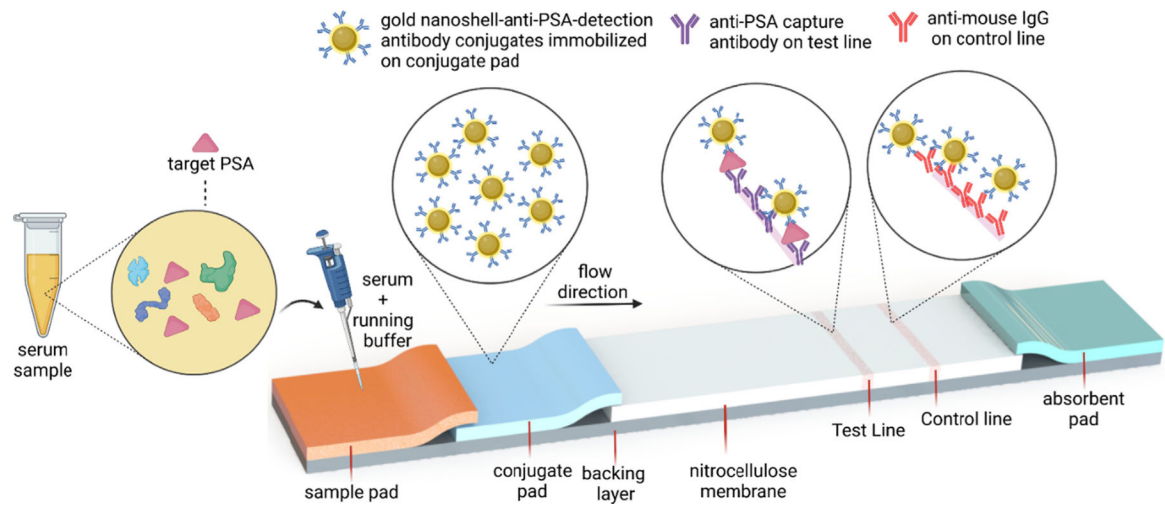


**Fig. 2.** Lateral flow test strip components with sandwich assay format for quantification of tPSA. Created with [BioRender.com](https://www.biorender.com).

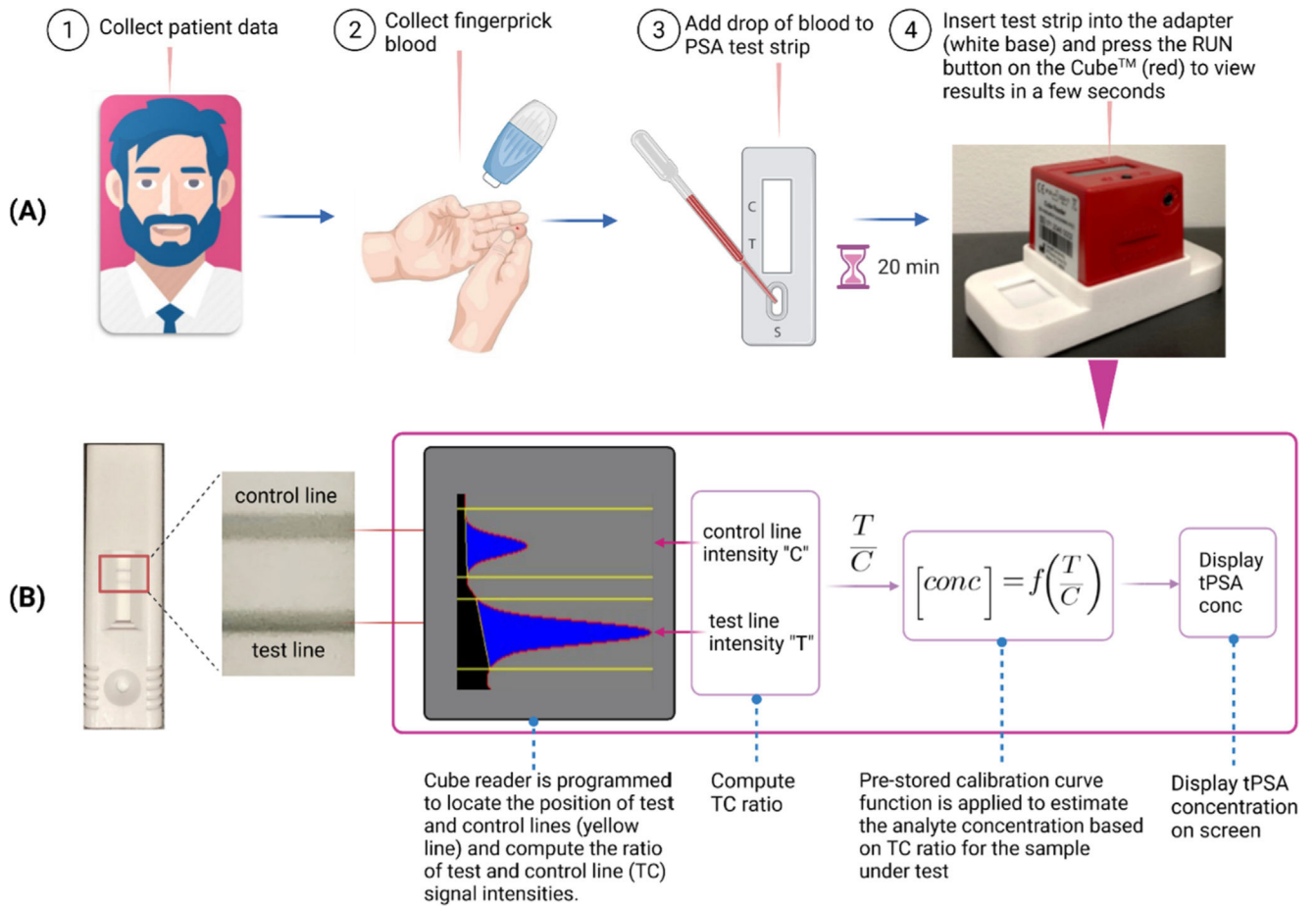


**Fig. 3.** (A) Schematic showing the testing protocol (B) main data processing steps within the Cube™ reader.

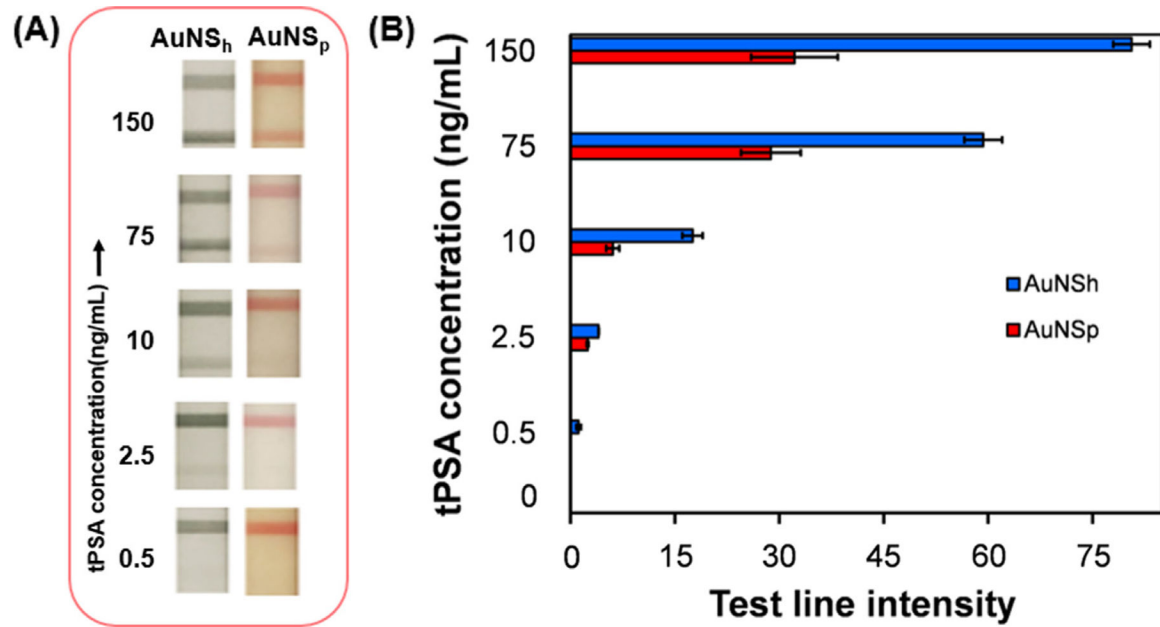


**Fig. 4.**  
 (A) Representative images of colorimetric changes of the test and control lines on the  $AuNS_h$  and  $AuNS_p$ -labeled versions of test strips for various tPSA calibrator concentrations  
 (B) Grouped bar chart where the x-axis indicates average test line intensities measured with Cube™ reader in  $AuNS_h$  and  $AuNS_p$ -labeled test strip pairs grouped by each tPSA calibrator concentration tested (shown on y-axis).

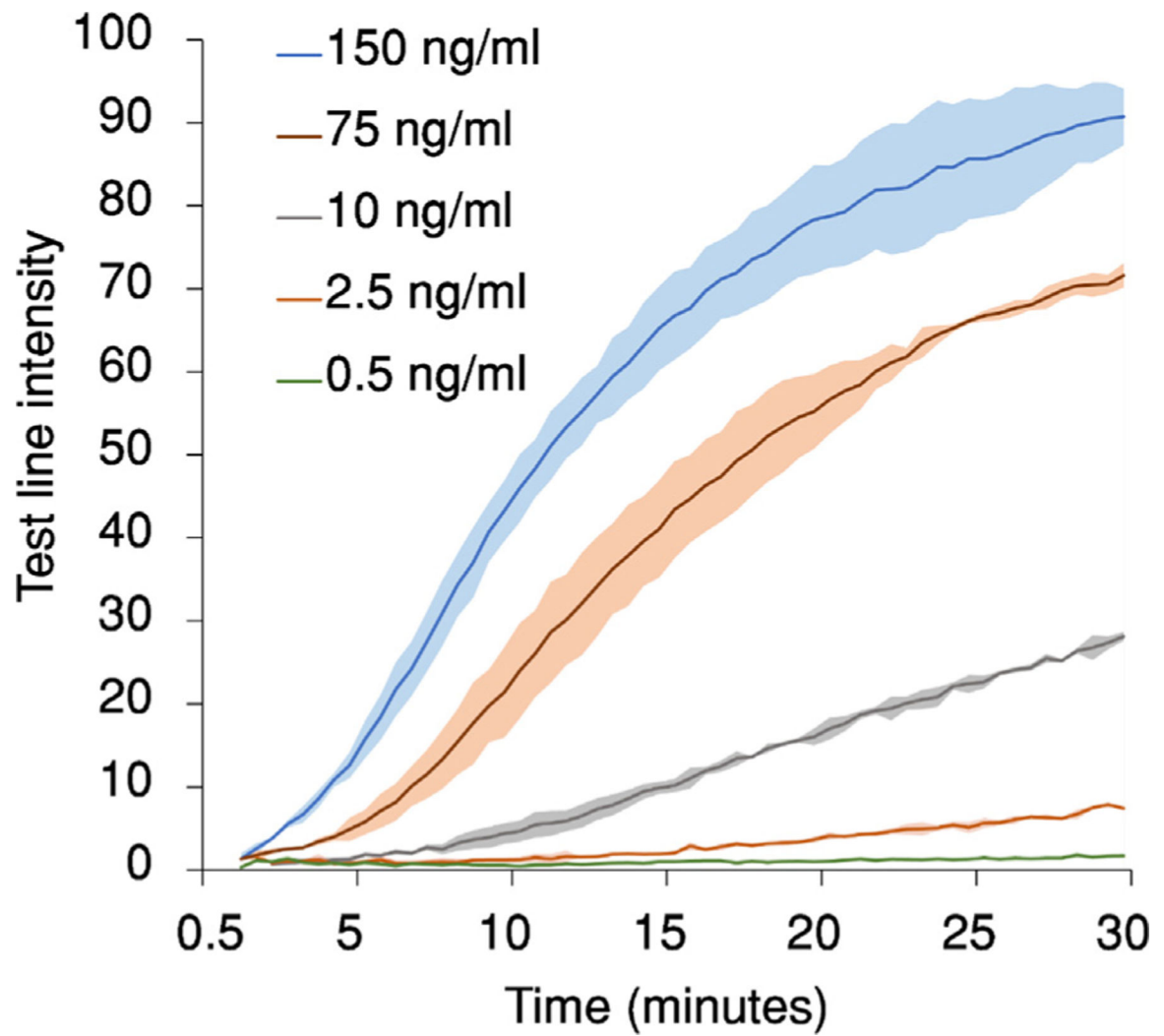


**Fig. 5.** Immunoreaction kinetics with test line intensities measured by Cube™ plotted on y-axis against time on x-axis, for each tPSA concentration from the calibration kit. Shaded region around the data line represents error bars based on standard deviation.

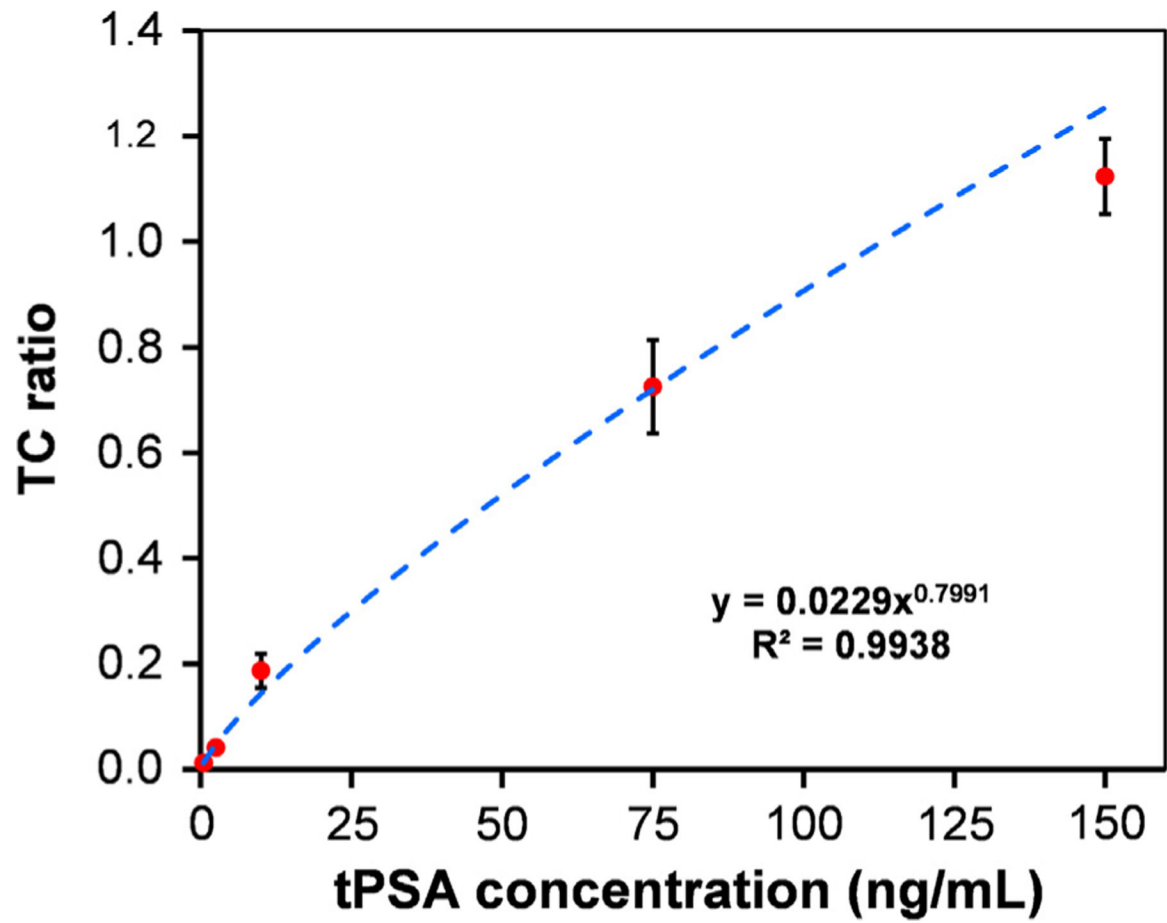


**Fig. 6.** Calibration curve fitted with a power model for TC ratio measured with Cube™ for AuNS<sub>h</sub>-labeled test strips tested with various concentrations of Access Hybritech PSA calibrator.

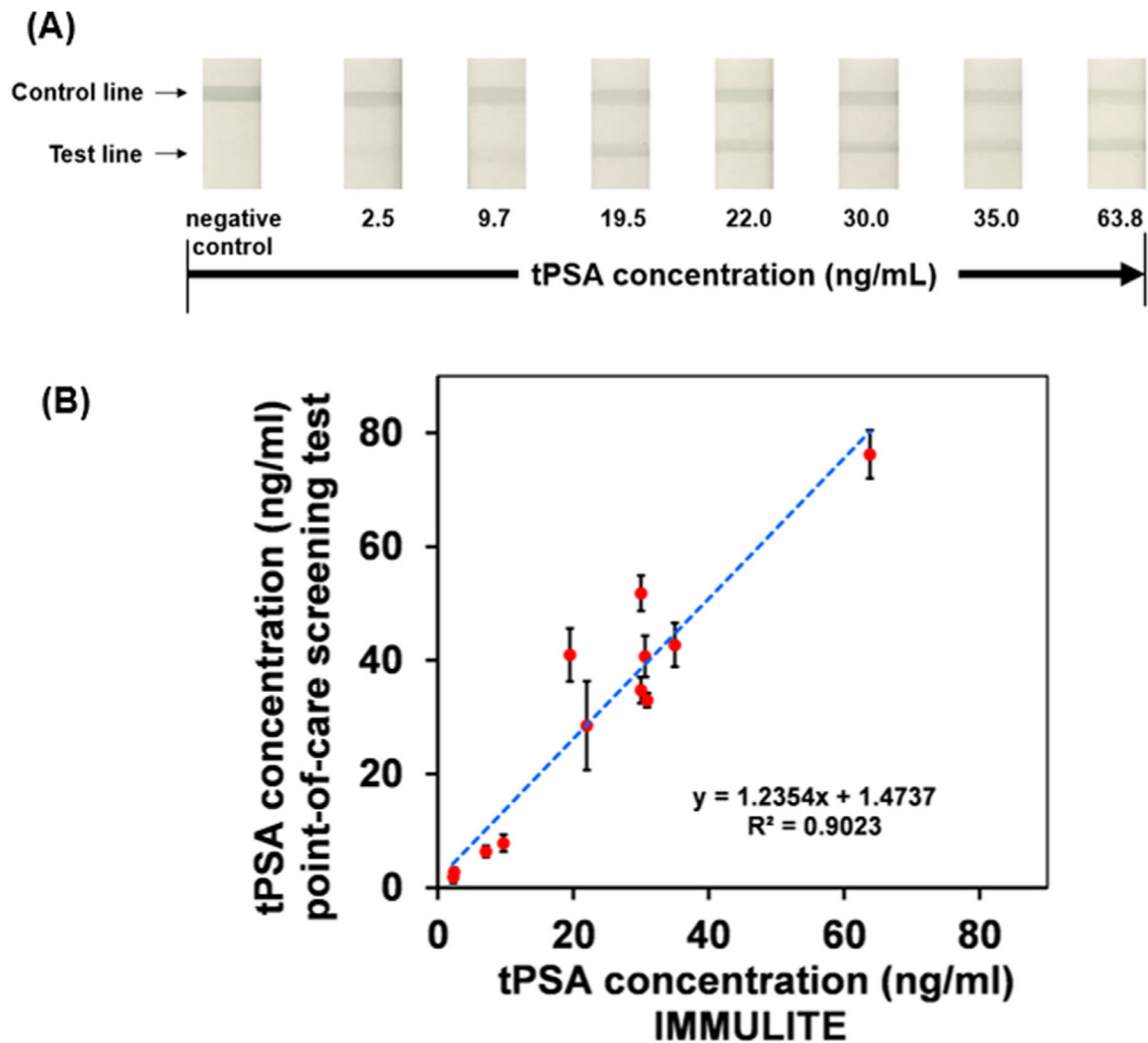


**Fig. 7.**

(A) Representative images of the colorimetric changes of the test and control lines on the test strip after test completion at various known concentrations of serum samples shown below each test strip image, in increasing order from left to right (B) Comparison of predicted tPSA concentrations from point-of-care approach on y-axis and tPSA concentrations quantified by IMMULITE method on the x-axis. Error bars represent standard deviations of predicted tPSA concentration results from serum samples assayed in triplicate. Simple linear regression was used to test if the point-of-care approach significantly predicted tPSA concentrations quantified by gold standard IMMULITE method.

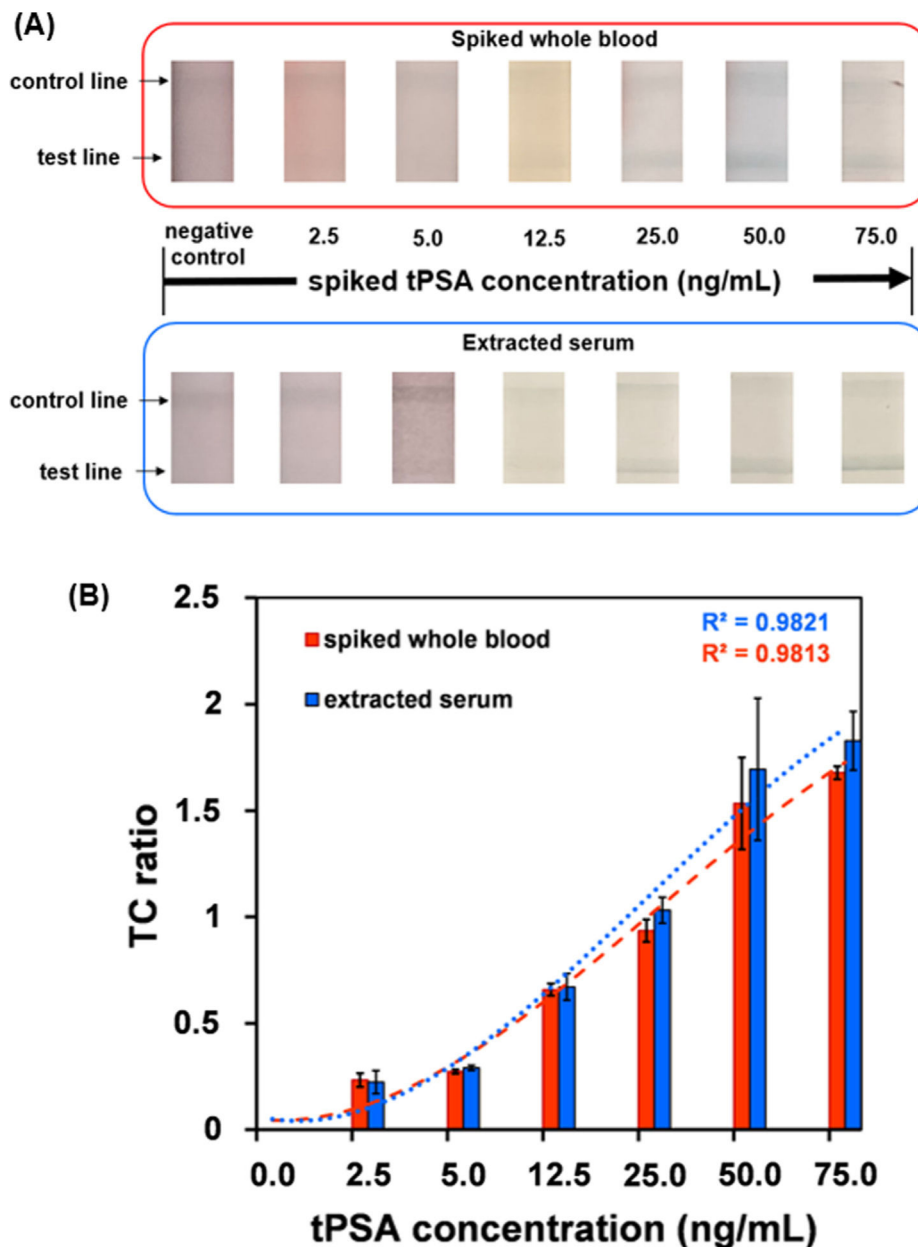


**Fig. 8.** (A) Representative images of the colorimetric changes of the test and control lines on the test strip after test completion at various tPSA concentrations of spiked whole blood samples (top row of images) and extracted serum samples (bottom row) (B) Grouped bar chart, where the x-axis indicates spiked tPSA concentrations and the y-axis indicates average test line intensities measured with Cube™ reader for spiked whole blood and extracted serum pairs for each spiked tPSA concentration tested. Red dashed and blue dotted line represent third order polynomial trendline fitted for spiked whole blood and extracted serum data, respectively.